Asian Journal of Applied Sciences



Mathematical Modeling of Reverse Osmosis Process by the Orthogonal Collocation on Finite Element Method

¹Belkacem Absar, ¹Sid El Mahi Lamine Kadi and ²Omar Belhamiti ¹Laboratoire d'Energie-Environnement et Développement Durable, Université de Mostaganem, 27000 Mostaganem, Algérie ²Laboratoire de Mathématiques Pures et Appliquées, Université de Mostaganem, 27000 Mostaganem, Algérie

Abstract: A simplified model is used to predict the performance of hollow fiber reverse osmosis membrane. The model is based on the solution-diffusion mass transfer model and takes into account the effect of the flow pattern of the permeate in the membrane. Two types of flow pattern can be distinguished: the co-current and counter-current flow pattern. The resolution of the mathematical model developed for the counter-current flow pattern is subject to the Boundary Value Problems (BVP). A convenient computational method is used to solve BVP using orthogonal collocation on finite elements. This method is the conjunction of Finite Element Method (FEM) and Orthogonal Collocation Method (OCM). OCM discretize BVP's conveniently where as FEM provides accuracy to the solution. The model is verified using experimental data from literature. Co-current and counter-current flow operations are compared using parameters of overall recovery, average product concentration and final feed concentration in closed loop process. The simulation results show that the operating time in the case of counter-current flow is longer than that of the co-current flow. Thus, the overall recovery is higher. These results show clearly the better efficiency of the counter-current flow pattern in the concentrating process.

Key words: Water desalination, reverse osmosis, co-current, counter-current, simulation, numerical resolution

INTRODUCTION

Reverse osmosis is a method of separation and concentration process in liquid phase. This process found a broad application in the desalination of sea and brackish water. It is applied to purify water for laboratory use and is very promising as a pre-concentration technique in trace and environmental analysis (Mariott and Sørensen, 2003). The major advantage of this process is that it can be performed at ambient temperature and does not require any energy for initial feed heating as it is the case of the distillation processes and no phase change is involved (Kahdim *et al.*, 2003).

The process consists in passing an aqueous solution under pressure through an appropriate membrane and withdrawing the membrane permeate at atmospheric pressure and ambient temperature. The product obtained is enriched in one of the mixture components. The other components are recovered in the retentate with higher concentration in the high-pressure side of the membrane. Many mathematical models were developed to describe the behavior of this process (Kahdim *et al.*, 2003; Mariott *et al.*, 2001; Fletcher and Wiley, 2004). These models also predict the performance of reverse osmosis units for better running. However, the majority of these studies considers only co-current flow and does not take account of counter-current flow.

This study proposes a simple and effective mathematical model for the hollow-fiber membrane modules. It takes account of the flow direction in the feed and the permeate side of the membrane. It enables to study together the co-current and the counter-current flow patterns.

The objective of this research is to determine the influence of the flow direction of feed flow (feed side) and permeate flow (fiber side) on the effectiveness of separation in a reverse osmosis module. The proposed model takes into account two types of flow pattern: the co-current and countercurrent flow patterns. This model is used to predict the performances of RO unit and compare them for the two types of flow pattern. The parameters used to achieve this comparison are the overall recovery and the purity rate.

The resolution of the mathematical model in the case of the counter-current flow pattern is confronted to the boundary value problems. This difficulty is overcome by the use of orthogonal collocation on finite element method.

In recent years, considerable attention has been focused on a class of direct transcription methods called pseudospectral or orthogonal collocation methods. The orthogonal collocation method on finite element method is a useful method for problems whose solution has steep gradients and the method can be applied to time-dependent problems, too.

The orthogonal collocation on finite elements method was used in several and various fields. Riascos and Pinto (2002) used this method in bioprocess dynamic optimization. They found that discretization of differential equations systems by orthogonal collocation in finite elements efficiently transforms dynamic optimization problems into nonlinear programming (NLP) problems, enabling to solve complex problems with several control variables and minimizing the approximation error. This method was also used by Lu (2004) in Mathematical modeling of salt-gradient ion-exchange simulated moving bed chromatography for protein separations. Araya *et al.* (2007) used this method in the Solid substrate fermentation mathematical modeling. They concluded that this method is fast, robust and reliable and had shown its suitability for fitting a variety of complex dynamic models.

In our approach, an iterative technique was developed to uncouple the system of the differential equations. The non linear problem is thus transformed from a non linear to a linear problem. This linearization allows more stability. The numerical resolution of the proposed mathematical model using this procedure has led to results with high precision (check of material balance with high precision).

DEVELOPMENT OF EQUATIONS

Many mechanistic and mathematical models have been proposed to describe reverse osmosis membranes. Models that adequately describe the performance of reverse osmosis membranes are very important since these are needed in the design of reverse osmosis units.

The model based on the solution-diffusion is the most used. It is based on the diffusion of the solvent and the solute through a membrane. This model supposes that both the solute and solvent dissolve at the membrane surface and diffuse across it. The solute and solvent diffusion is uncoupled and is due to the chemical potential gradient across the membrane. These gradients are the result of concentration and pressure differences across the membrane.

Solvent and Solute Transport Equations

The solvent mass flux J_{w} , which is generally water, can be expressed by Fick's law. It depends on ΔP , the pressure difference across the membrane and the osmotic pressure difference of the solution across the membrane (Al-Bastaki and Abbes, 1999, 2000):

$$J_{w} = A_{w} (\Delta P - \Delta \pi) \tag{1}$$

where, A_w is the water permeability constant.

The difference in osmotic pressure $\Delta \pi$ on both sides of the membrane is expressed as:

$$\Delta \pi = \pi_{\rm F} - \pi_{\rm p} \tag{2}$$

where, the subscript F refers to the feed side and the subscript P to the permeate side.

For not too high a solute concentration, the osmotic pressure is approximately a linear function of solute concentrations (Al-Bastaki and Abbes, 2004; Senthilmurugan *et al.*, 2005):

$$\pi = \alpha C \tag{3}$$

where, α is a proportionality coefficient (Abbes, 2005). By substituting Eq. 3 into Eq. 1 we obtain:

$$J_{w} = A_{w} \left(\Delta P - \alpha \Delta C \right) \tag{4}$$

where, ΔC is the difference of the solute concentration across the membrane, expressed as:

$$\Delta C = C_{F} - C_{p} \tag{5}$$

where, C_F and C_P are the concentrations in the feed and permeate side, respectively.

The volumetric flow rate can be expressed as:

$$Q_{w} = \frac{J_{w}Sa}{\rho_{w}} \tag{6}$$

where, Sa is the membrane surface area and ρ_w is the water density.

For the solute flux it is assumed that the chemical potential difference due to pressure is negligible and so the driving force is almost entirely due to concentration differences. From Fick's law, the solute mass flux is:

$$J_{s} = B_{s}(\Delta C) \tag{7}$$

where, B_s the solute permeability coefficient which is a function of the solute composition and membrane structure.

The solute mass flow rate is expressed as:

$$\overset{\bullet}{Q}_{s} = J_{s}Sa = B_{s}Sa\left(C_{F} - C_{P}\right) \tag{8}$$

The membrane rejection is defined as the fraction of solute present in the solution which is stopped by the membrane:

$$T_{R} = \frac{C_{F} - C_{P}}{C_{F}} = 1 - \frac{C_{P}}{C_{F}} \tag{9}$$

Using the relations for solvent and solute flux, solute rejection for the solution-diffusion model can be expressed as:

$$\frac{1}{T_{_{\!R}}} = 1 + \frac{B_{_{\!S}}\rho_{_{\!W}}}{A_{_{_{\!W}}}} \left(\frac{1}{\Delta P - \Delta \pi}\right) \tag{10}$$

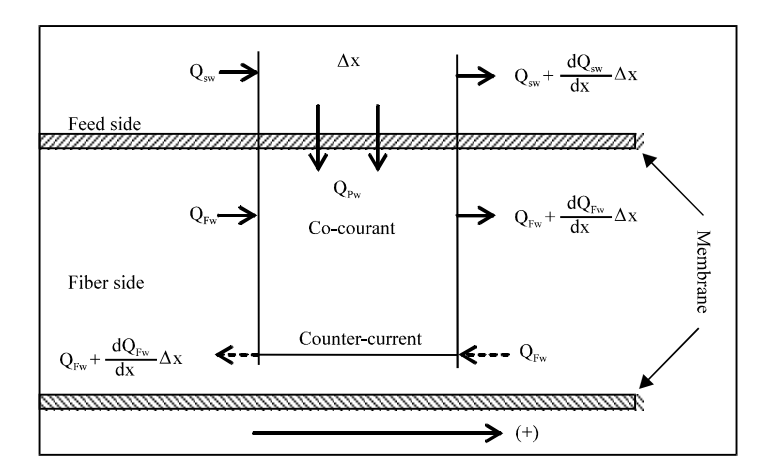


Fig. 1: Flow rate change across Δx

For large pressure values, solute rejection approaches unity.

Other parameters are defined to determine the performances of a reverse osmosis system. The water recovery is a production term which relates permeate and feed flows. This factor is function of time and expressed as:

$$WR_{t} = \frac{Q_{p}}{Q_{F}} \tag{11}$$

For the overall system, recovery can be defined as the permeate production divided by the initial feed volume. This is used in the closed loop batch concentrating mode. This term is not a function of time, its expression is:

$$WR_{ov} = \frac{V_{P}}{V_{F}^{0}} \tag{12}$$

Hollow Fiber Membrane Mathematical Model

The most widely used membrane modules are the spiral-wound and hollow fiber elements. A hollow fiber module contains a large number of membranes fibers housed in a module shell. The feed can be introduced either on the shell side or on the fiber side. Permeate is usually withdrawn in a co-current or counter-current manner, with the latter being generally more effective (Mariott and Sørensen, 2003). The flow patterns for both the co-and counter-current flow are shown in Fig. 1.

Co-Current Flow Pattern

In this flow pattern, the permeate and the feed in the fiber side and the shell respectively, flow co-currently. According to the solution-diffusion model, the rate of permeate in an elemental section length Δx for water is:

$$Q_{pw} = \frac{A_{w}}{\rho_{w}} (\pi D_{m} \Delta x) (\Delta P - \alpha (C_{F} - C_{P}))$$
(13)

where, $\boldsymbol{D}_{\!\scriptscriptstyle m}$ is the mean diameter

The material balance for water in the shell side is obtained:

$$Q_{pw} = \left(Q_{sw} + \frac{dQ_{sw}}{dx}\Delta x\right) + Q_{pw}$$
 (14)

where, Q_{sw} is the water volumetric flow rate in the shell side (Fig. 1). The first subscript indicates the shell or the fiber side and the second subscript indicates the solute or the water.

This equation reduces to:

$$\frac{dQ_{gw}}{dx} = -\frac{Q_{gw}}{\Delta x} \tag{15}$$

Substituting for Q_{pw} in Eq. 13:

$$\frac{dQ_{_{sw}}}{dx} = -\frac{A_{_{w}}}{\rho_{_{w}}} \left(\pi D_{_{m}}\right) \left(\Delta P - \alpha \left(C_{_{F}} - C_{_{P}}\right)\right) \tag{16} \label{eq:16}$$

 C_F indicates the solute concentration in the feed flow rate (shell side). It is expressed as the ratio of the solute mass flow rate on the water volumetric flow rate:

$$C_{F} = \frac{\dot{Q}_{ss}}{Q_{crv}} \tag{17}$$

 $Q_{\mbox{\tiny SS}}$: Solute mass flow rate in the shell side.

Similar equation is obtained for the solute concentration C_p in the permeate flow rate (fiber side):

$$C_p = \frac{\dot{Q}_{fs}}{Q_{s-}} \tag{18}$$

where, \dot{Q}_{fs} and Q_{fw} are respectively, the solute mass flow rate and the water volumetric flow rate in the fiber side.

Equation 16 becomes:

$$\frac{dQ_{sw}}{dx} = -\frac{A_{w}}{\rho_{w}} \left(\pi D_{m}\right) \left(\Delta P - \alpha \left(\frac{\dot{Q}_{ss}}{Q_{sw}} - \frac{\dot{Q}_{fs}}{Q_{fw}}\right)\right)$$
(19)

The material balance for water on the fiber side is obtained in the same manner:

$$\frac{dQ_{\text{fiw}}}{dx} = \frac{A_{\text{w}}}{\rho_{\text{w}}} \left(\pi D_{\text{m}}\right) \left(\Delta P - \alpha \left(\frac{\dot{\mathbf{Q}}_{\text{ss}}}{Q_{\text{sw}}} - \frac{\dot{\mathbf{Q}}_{\text{fs}}}{Q_{\text{fw}}}\right)\right) \tag{20}$$

The material balance for the solute in the shell side gives (Fig. 1):

$$\vec{Q}_{ss} = \left(\vec{Q}_{ss} + \frac{d\vec{Q}_{ss}}{dx}\Delta x\right) + \vec{Q}_{ps}$$
 (21)

where, \dot{Q}_{ss} is the solute mass flow rate in the shell side and \dot{Q}_{ps} the solute mass flow rate across the membrane

Arranging this equation and substituting Q_{ns} by its expression Eq. 8 gives:

$$\frac{d\dot{Q}_{ss}}{dx} = -B_s \left(\pi D_m\right) \left(\frac{\dot{Q}_{ss}}{Q_{sw}} - \frac{\dot{Q}_{fs}}{Q_{fw}}\right)$$
(22)

A similar equation is obtained for the fiber side:

$$\frac{d\dot{Q}_{fs}}{dx} = B_s \left(\pi D_m\right) \left(\frac{\dot{Q}_{ss}}{Q_{sw}} - \frac{\dot{Q}_{fs}}{Q_{fw}}\right)$$
(23)

Finally, the mathematical model obtained is composed of a set of four ordinary differential equations:

$$\begin{cases} \frac{dQ_{\text{gw}}}{dx} = -\frac{\pi D_{\text{m}} A_{\text{w}}}{\rho_{\text{w}}} \left(\Delta P - \alpha \left(\frac{\dot{Q}_{\text{gg}}}{Q_{\text{gw}}} - \frac{\dot{Q}_{\text{fg}}}{Q_{\text{fw}}} \right) \right) \\ \frac{dQ_{\text{fw}}}{dx} = \frac{\pi D_{\text{m}} A_{\text{w}}}{\rho_{\text{w}}} \left(\Delta P - \alpha \left(\frac{\dot{Q}_{\text{sg}}}{Q_{\text{gw}}} - \frac{\dot{Q}_{\text{fg}}}{Q_{\text{fw}}} \right) \right) \\ \frac{d\dot{Q}_{\text{gg}}}{dx} = -\pi D_{\text{m}} B_{\text{g}} \left(\frac{\dot{Q}_{\text{gg}}}{Q_{\text{gw}}} - \frac{\dot{Q}_{\text{fg}}}{Q_{\text{fw}}} \right) \\ \frac{d\dot{Q}_{\text{fg}}}{dx} = \pi D_{\text{m}} B_{\text{g}} \left(\frac{\dot{Q}_{\text{sg}}}{Q_{\text{gw}}} - \frac{\dot{Q}_{\text{fg}}}{Q_{\text{fw}}} \right) \end{cases}$$

$$(24a)$$

To determine the permeate flow rate at the end of the module, the ordinary differential equations in Eq. 24a must be integrated simultaneously.

Counter-Current Flow Pattern

In this flow pattern, the permeate and the feed in the fiber side and the shell side respectively, flow counter-currently. Proceeding in the same manner as for the co-current flow, we obtain analogous equations:

$$\begin{cases} \frac{dQ_{\text{gw}}}{dx} = -\frac{\pi D_{\text{m}} A_{\text{w}}}{\rho_{\text{w}}} \left(\Delta P - \alpha \left(\frac{\overset{\bullet}{Q}_{\text{gs}}}{Q_{\text{gw}}} - \overset{\bullet}{Q}_{f_{\text{g}}}}{Q_{f_{\text{w}}}} \right) \right) \\ \frac{dQ_{f_{\text{w}}}}{dx} = -\frac{\pi D_{\text{m}} A_{\text{w}}}{\rho_{\text{w}}} \left(\Delta P - \alpha \left(\frac{\overset{\bullet}{Q}_{\text{gs}}}{Q_{\text{gw}}} - \overset{\bullet}{Q}_{f_{\text{g}}}}{Q_{f_{\text{w}}}} \right) \right) \\ \frac{d\overset{\bullet}{Q}_{\text{gg}}}{dx} = -\pi D_{\text{m}} B_{\text{g}} \left(\overset{\bullet}{Q}_{g_{\text{gg}}} - \overset{\bullet}{Q}_{f_{\text{g}}}}{Q_{f_{\text{w}}} \right) \\ \frac{d\overset{\bullet}{Q}_{f_{\text{g}}}}{dx} = -\pi D_{\text{m}} B_{\text{g}} \left(\overset{\bullet}{Q}_{g_{\text{gg}}} - \overset{\bullet}{Q}_{f_{\text{g}}}}{Q_{f_{\text{w}}}} \right) \end{cases}$$

$$(24b)$$

These equations constitute the mathematical model for a counter-current flow pattern.

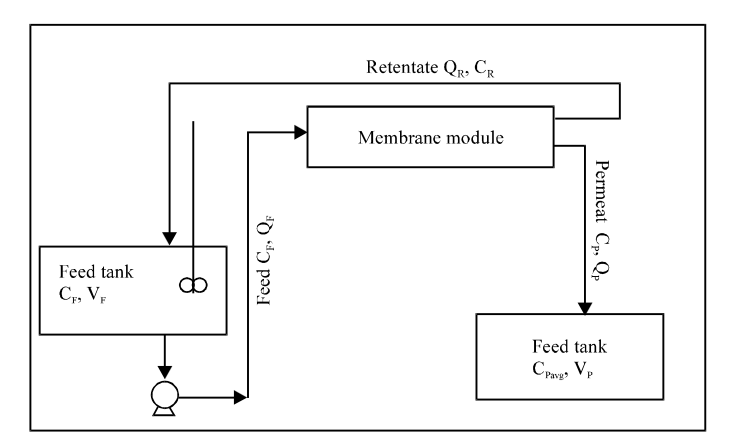


Fig. 2: Schematic diagram of reverse osmosis system

The models presented in this study describe ideal mass transfer and do not take account of the concentration polarization which is the accumulation of rejected solute at the surface of the membrane and can be minimized by increasing the feed velocity (Al-Bastaki and Abbes, 2004).

Process Modeling

Figure 2 shows the reverse osmosis system in continuous mode operation. It consists of a feed tank, a product tank and the membrane module. The retentate is recycled to the feed tank and the permeate is collected separately in the product tank. This process is used essentially in concentrating system (Slater *et al.*, 1985; Slater and Brooks, 1992; Jamal *et al.*, 2004).

The material balance equation applied to product tank yields:

$$Q_{p} C_{p} = \frac{d(V_{p} C_{Pavg})}{dt}$$
 (25)

 C_{Parg} is the average concentration of the obtained product and its volume after a defined time of running.

Development of this equation gives:

$$Q_{p}C_{p} = V_{p}\frac{dC_{psvg}}{dt} + C_{Pavg}\frac{dV_{p}}{dt} \tag{26} \label{eq:26}$$

with initial conditions: at t=0, $V_p=0$, $C_{Pavg}=C_P=0$. The change in the volume of product corresponds to the production rate of the membrane:

$$\frac{dV_{_{p}}}{dt}=Q_{_{p}} \tag{27}$$

Substitution into Eq. 26:

$$\frac{dC_{pavg}}{dt} = \frac{Q_p \left(C_p - C_{pavg}\right)}{V_n} \tag{28}$$

The material balance on the membrane module yields:

Asian J. Applied Sci., 1 (1): 1-18, 2008

$$Q_F C_F = Q_P C_P + Q_R C_R$$
 (29)

Similar material balance equation can be obtained around the feed tank:

$$Q_R C_R - Q_F C_F = \frac{d(V_{Ft} C_{Ft})}{dt}$$
(30)

Developing this equation yields:

$$-Q_{p}C_{p} = V_{pt}\frac{dC_{pt}}{dt} + C_{pt}\frac{dV_{pt}}{dt}$$
(31)

where, V_{Ft} is the volume in the feed tank at a time t, with a concentration inside the tank C_{Ft} . The feed tank is assumed well mixed. Thus the concentration of the feed to the membrane module is equal to the concentration in the feed tank:

$$V_{p_t} = V_p \tag{32}$$

and

$$C_{p_t} = C_p \tag{33}$$

The change volume in the feed tank with time corresponds to the production rate:

$$-\frac{dV_p}{dt} = Q_p \tag{34}$$

Integrating this equation with initial conditions: at t = 0, $V_F = V_F^0$

$$V_{F} = V_{F}^{0} - Q_{P} t {35}$$

Substituting these expressions in Eq. 30:

$$\frac{dC_F}{dt} = \frac{Q_P \left(C_F - C_P\right)}{\left(V_F^0 - Q_P t\right)} \tag{36}$$

One parameter of interest is the overall recovery, WR_{ov}, which can be obtained by using Eq. 12.

Knowing that the operating system is closed, the mass conservation implies that the mass of the solute in the feed tank at initial time is equal to the sum of the various streams and tanks. So:

$$V_{p} = \frac{V_{p}^{0} \left(C_{F} - C_{F}^{0}\right)}{C_{F} - C_{perg}}$$
(37)

Substituting V_P by its expression in Eq. 28:

$$\frac{dC_{\text{pavg}}}{dt} = \frac{Q_{\text{p}}\left(C_{\text{p}} - C_{\text{pavg}}\right)}{V_{\text{p}}^{0}\left(C_{\text{F}} - C_{\text{p}}^{0}\right)} \left(C_{\text{F}} - C_{\text{pavg}}\right) \tag{38}$$

Equation 36 and 38 are the result of material balances on the feed tank, product tank and the membranes module. The resolution of this set of two ordinary differential equations requires the values of C_P and Q_P . These values are obtained by integrating the set of ordinary differential equations developed above for co-current or counter-current flow.

The solution of Eq. 36 provides the concentration feed as function of the operating time. The solution of Eq. 38 provides the average concentration of the solute in product tank and the water volume by using Eq. 37. Equation 12 gives the value of the water overall recovery.

METHODS OF RESOLUTION

The method of orthogonal collocation as described by Villadsen and Michelsen (1978), can lead to the numerical resolution of many problems. However, it does not prove very effective for certain cases where the solution is very irregular. To avoid this problem, it is necessary to take a very great order of approximation. It is a disadvantage which limits the application fields of this technique. This is the reason why the orthogonal collocation method is combined with the finite element method.

In this study, the orthogonal collocation on the finite element method as a numerical method to solve the boundary value problems is chosen due to its efficiency and robustness.

Tessendorf *et al.* (1999) have used the orthogonal collocation on finite element method to solve a non linear equation. Gauss Method was used to solve the non linear algebraic equation.

An initial profile of solution for each equation is given, which verifies the boundary conditions, $y_1^{(1)}$, $y_2^{(1)}$, $y_3^{(1)}$, $y_3^{(1)}$, $y_4^{(1)}$. The iterative procedure can be written as:

$$\begin{cases} \frac{dy_{1}^{(k+1)}}{dx} = f_{1}\left(x, y_{1}^{(k)}, y_{2}^{(k)}, y_{3}^{(k)}, y_{4}^{(k)}\right) \\ \frac{dy_{2}^{(k+1)}}{dx} = f_{2}\left(x, y_{1}^{(k+1)}, y_{2}^{(k)}, y_{3}^{(k)}, y_{4}^{(k)}\right) \\ \frac{dy_{3}^{(k+1)}}{dx} = f_{3}\left(x, y_{1}^{(k+1)}, y_{2}^{(k+1)}, y_{3}^{(k)}, y_{4}^{(k)}\right) \\ \frac{dy_{4}^{(k+1)}}{dx} = f_{4}\left(x, y_{1}^{(k+1)}, y_{2}^{(k+1)}, y_{3}^{(k+1)}, y_{3}^{(k)}\right) \end{cases}$$

$$(39)$$

where, $y_i^{(k+1)}$ and $y_i^{(k)}$ are the approximations of the solution y_i at the current and the precedent iteration, respectively.

At each iteration, the orthogonal collocation on the finite element method is applied to each linear differential equation (Fig. 3). Thereafter we can calculate the uncoupling error by using the following formula:

$$Error = Max(\|y_1^{(k+1)} - y_1^{(k)}\|, \|y_2^{(k+1)} - y_2^{(k)}\|, \|y_3^{(k+1)} - y_3^{(k)}\|, \|y_4^{(k+1)} - y_4^{(k)}\|) \tag{40}$$

This procedure gives the solution of the problem, when the error is under a given small epsilon.

To explain the procedure, we consider the below differential equation in the domain Ω :

$$y'(x) + a(x)y(x) = f(x)$$
 (41)

The domain Ω is divided into n elements. After that, the orthogonal collocation is applied in each element $(\Omega^{(i)})_{i=1.n}$.

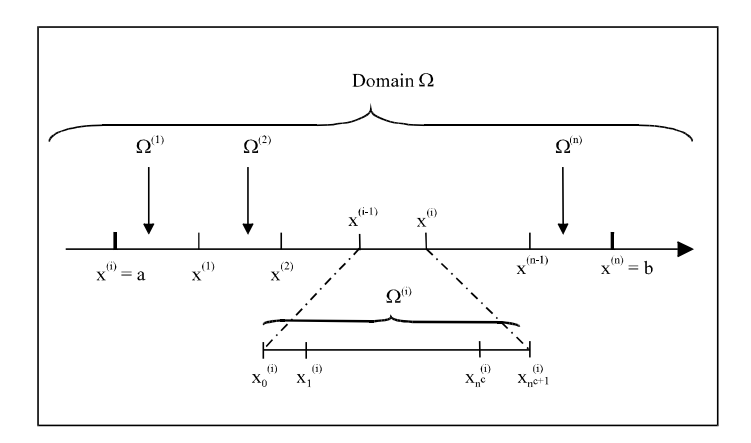


Fig. 3: Finite element collocation discretization

The elementary solution of Eq. 41 in the ith element is given by:

$$y^{(i)}(x) = \sum_{i=0}^{n^{c}+1} y_{j}^{(i)} l_{j}(x)$$
 (42)

where, n^c is the number of internal collocation points and $l_j(x)$ is the j^{th} degree Lagrange polynomials. Substitution of Eq. 42 into Eq. 41 generates residual:

$$R(x) = \frac{d y^{(i)}(x)}{d x} + a(x) y^{(i)}(x) - f(x)$$
 (43)

The weighted functions are then used to reduce the residual to a minimum value:

$$\psi_{j}\!\left(x\right)\!=\!\!\left\{ \begin{array}{ll} 1 & \text{for } x=\!x_{j}^{\text{c}} \\ 0 & \text{for } x\neq\!x_{j}^{\text{c}} \end{array} \right. \qquad \text{for } j=0..n^{\text{c}}\!+\!1 \eqno(44)$$

and

$$\sum_{x_{0}^{(i)}}^{x_{n-1}^{(i)}} R(x) \psi_{j}(x) dx = 0$$
 (45)

Consequently:

$$R(\mathbf{x}_i^c) = 0 \tag{46}$$

Substituting the expressions of $\frac{dy^{(i)}}{dx}(x_j^e)$ and $y^{(i)}(x_j^e)$ in Eq. 46 leads to a linear system with (n^e+2) equations and (n^e+2) unknowns:

$$\mathbf{M}^{(i)} \mathbf{y}^{(i)} = \mathbf{b}^{(i)} \tag{47}$$

 $M^{(i)}$ and $b^{(i)}$ are the elementary matrix and its second member in the ith element $\Omega^{(i)}$

By applying the same procedure to each element $(\Omega^{(i)})_{i=1..n}$ n systems of algebraic linear equations are obtained. These linear systems are assembled into a global system expressed as follows:

$$M^{G} y = b^{G}$$
 (48)

where, M^G and b^G are the global matrix and its second member. The vector y represents the global solution of Eq. 41 on Ω .

MODEL VERIFICATION

The presented model was verified using experimental data from references (Slater and Brooks, 1992). The experimental results were extracted and plotted as a function of time for comparison with simulation results using the proposed mathematical model. The membrane specifications and the operating parameters are given in Table 1.

RESULTS AND DISCUSSION

Two simulations were run using the data from Table 1, first to verify the proposed mathematical model validity, then to compare the co-current and counter-current flow pattern performances.

Mathematical Models and Experimental Data Comparison

The first experimental run to which the mathematical model was tested utilizes a NaCl aqueous solution. The experimental system consists of a tubular cellulose acetate membrane with a hydraulic difference pressure applied across the membrane of 4.02×10^{13} kg m⁻¹ h². The reverse osmosis unit was operated for 30 h (Slater and Brooks, 1992) whereas the simulation can be carried out up to 140 h.

Only limited experimental data are available. Therefore, no comparison between experimental and simulated data could be made beyond 30 h time. A comparison is also made between the simulation results of the proposed model and those obtained by the model suggested by Slater and Brooks (1992). The simulation with Slater and Brooks model can run for only 129 h.

Figure 4 shows the variation of solute feed concentrations with time. Three areas can be distinguished. Initially, the feed concentration increases slightly with time. The small recycled quantity of the more and more concentrated retentate has a little influence on the tank feed concentration. The linearity observed in the early hours of the simulation is based on the initial volume in the feed tank. Larger values of would leave the curve linear much longer. Beyond 40 h, the feed concentration increases gradually with time. Because of permeate production; the feed volume continuously decreases with time resulting in an increase of feed concentration with time. At the end of operation, the solvent flux across the membrane is very low due to an increase in the osmotic pressure. The volume and the concentration of the feed tank vary slightly with time.

Table 1: Operating parameters value

Parameters	Values
Initial feed concentration (C _F ⁰)	2.0 kg m ⁻³
Initial volume in the feed tank (V _F ⁰)	$0.15 \mathrm{m}^{3}$
Membrane surface area (Sa)	0.181 m^2
Water density (ρ_w)	$1000 \mathrm{kg} \mathrm{m}^{-3}$
Transmembrane pressure (ΔP)	$4.02 \times 10^{13} \text{ kg m}^{-1} \text{ h}^2$
Proportionality coefficient (α)	$1.02 \times 10^{12} \text{ m}^2 \text{ h}^{-2}$
Water permeability constant (A _w)	$4.20 \times 10^{-13} \mathrm{h} \;\mathrm{m}^{-1}$
Solute permeability coefficient (B _s)	$1.12 \times 10^{-4} \mathrm{m}h^{-1}$

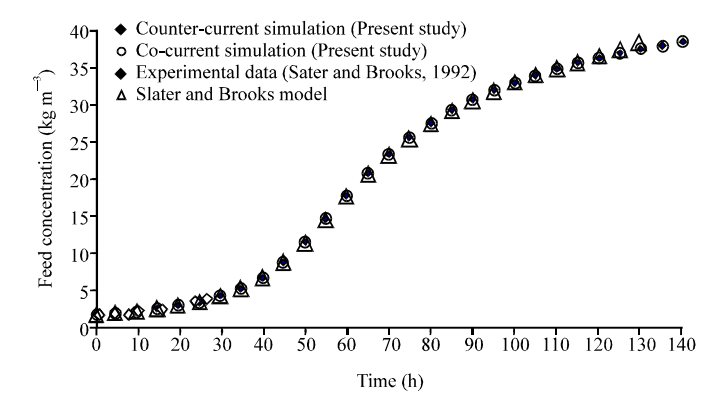


Fig. 4: Simulation results of solute feed concentration vs. time in the co- and counter-current flow patterns

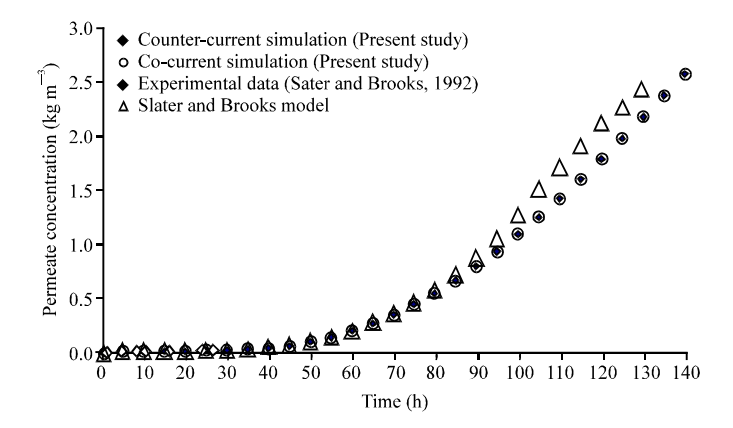


Fig. 5: Simulation results of solute concentration in the permeate vs. time in the co- and countercurrent flow patterns

The results obtained by simulation are in good agreement with the experimental data for the first 30 h. Beyond this time, the simulation results, which represent only a prediction, are also in good agreement with those obtained by using the model proposed by Slater and Brooks (1992). The results simulation for the co-current and the counter-current are similar and the corresponding curves are superposed.

Figure 5 shows the solute concentration in the permeate as a function of time. At the start of the operation, the permeate concentration is practically constant. This is due to the small variation in the feed concentration. Beyond 50 h, the change in the permeate concentration is more significant, reaching $2.66~\rm kg~m^{-3}$ at the end of simulation. The simulation results for both co-current and counter-current agree again with experimental data for the first 30 h time. The two models results are in good agreement and deviate at the end of the simulation. Similar behavior is observed for the counter-current and the co-current flow pattern.

A parameter of a great importance is the averages permeate concentration. It indicates the purity rate of the final product. The simulation results again agree well with the available experimental data. The increase of the product average concentration with time is less significant because of the dilution effect in the product tank (Fig. 6). It reaches a value of 0.34 kg m⁻³ at the end of the simulation. As before, the two models simulation results behave in the same manner.

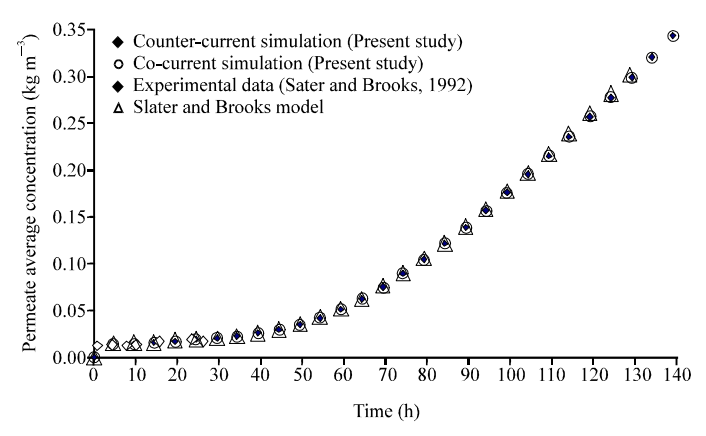


Fig. 6: Simulation results of solute concentration in the product tank vs. time in the co- and countercurrent flow pattern

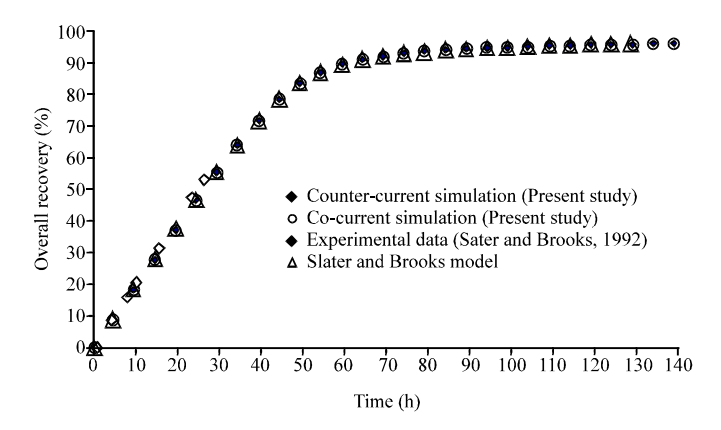


Fig. 7: Simulation results of overall recovery vs. time in the co- and counter-current flow patterns

This parameter has similar behavior in the counter-current and the co-current flow patterns. As predicted by the model, the overall recovery increases linearly with time up to 60 h (Fig. 7). Beyond this time, the increase is slightly constant due to a decrease in the solvent flux caused by an increase in the osmotic pressure. The overall recovery reaches a value of 0.95 at the end of the simulation.

Co-Current and Counter-Current Comparison

The mathematical model was used to compare the counter-current and co-current performances. The module with a co-current flow can operate only during 145.5 h. Beyond this time, the feed concentration becomes so significant and consequently the osmotic pressure, that the transmembrane pressure cannot overcome it. The module with a counter-current flow can operate longer. It reaches a value 152.5 h, which represents an additional time of 7 h of additional separation.

As shown in Table 2, the prolongation of the operating time improves the separation efficiency by increasing the overall recovery. However the concentration of the product increases, reaching a value of 0.39 kg m^3 .

As shown in Fig. 8, the feed concentration in the counter-current flow pattern reaches values larger than those obtained in the co-current flow pattern: 39.46 and 38.92 kg m⁻³, respectively. This is due to the recycling of the retentate which becomes more and more concentrated.

Table 2: Simulation results for the counter-current and the co-current flow patterns

Parameters	Co-current	Counter-current
Operating time (h)	145.50	152.50
Feed concentration (kg m ⁻³)	38.92	39.46
Average product concentration (kg m ⁻³)	0.37	0.39
Overall recovery (%)	95.77	95.90

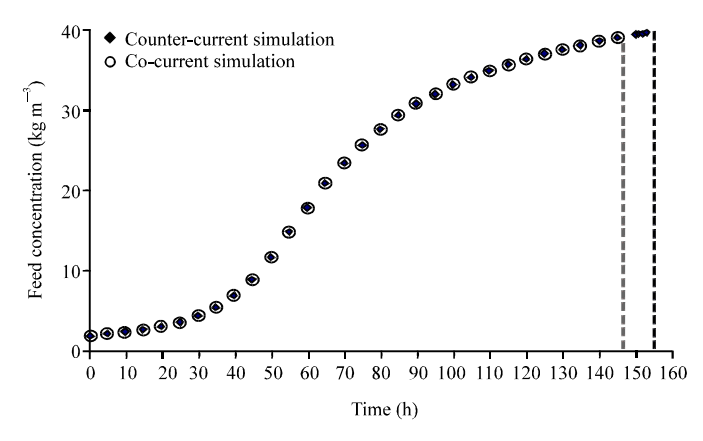


Fig. 8: Solute feed concentration vs. operating time in the co- and counter-current flow pattern

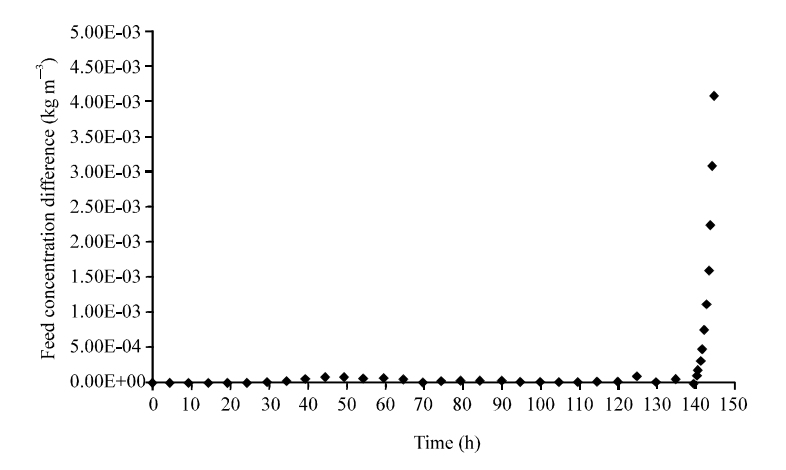


Fig. 9: Difference between the feed concentration values in the counter-current and the co-current flow pattern vs. time

The use of the counter-current flow pattern in reverse osmosis appears more interesting in the concentrating processes.

To investigate the behavior of the two types of flow pattern, the differences between the feed concentration values in both cases (feed concentration in the counter-current minus feed concentration in the co-current) were computed and plotted with time. The results obtained are shown in Fig. 9. The difference of the feed concentration values is very close to zero. However, after 140 h, this value increases abruptly. This is explained by the fact that beyond this time, the improvement of the feed concentration values in the case of the counter-current flow is more significant than that of the co-current flow pattern.

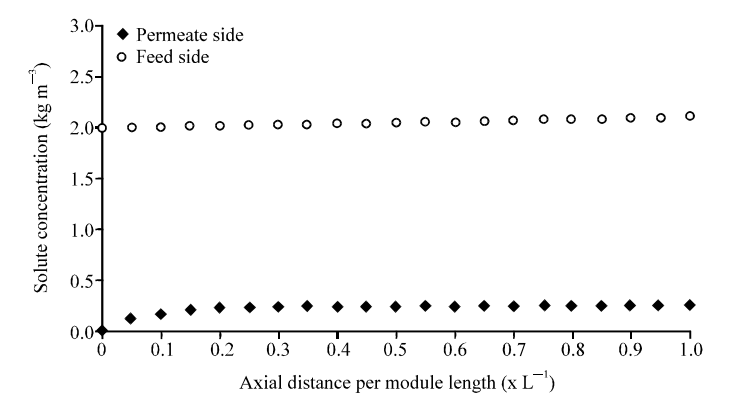


Fig. 10: Solute concentration along the module length (co-courant flow pattern)

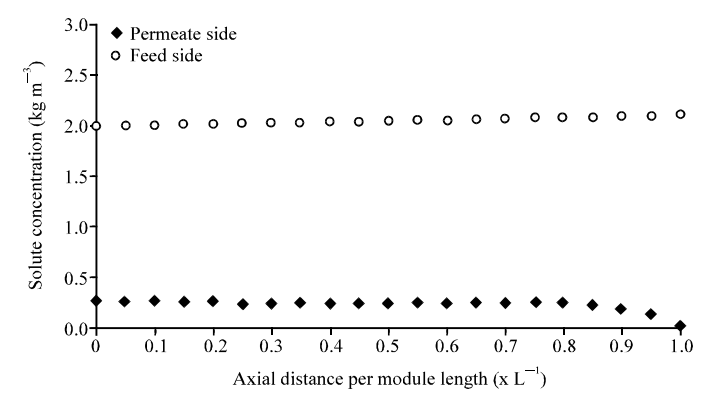


Fig. 11: Solute concentration along the module length (counter-courant flow pattern)

To explain the similarity obtained between the co-current and the counter-current simulation results, the solute concentration in the feed side and the permeate side are plotted versus the axial distance within the reverse osmosis module.

Equation 4 gives the relationship between the solvent flux across the membrane and the difference of the solute concentration on both sides of the membrane. The solvent flux across the membrane depends on three parameters:

- Membrane permeability of the solvent
- · Hydraulic pressure difference on both sides of the membrane
- Osmotic pressure difference on both sides of the membrane.

For a given separation, the two first parameters remain unchanged in both types of flow pattern: co-current or counter-current. The difference lies in the osmotic pressure difference that expresses the difference of solute concentration on both sides of the membrane. The solvent flux therefore depends on the solute concentration difference on both sides of the membrane. For a given hydraulic difference pressure, the solvent flux increases with the decrease in the difference of the solute concentration on both sides of the membrane.

As shown in Fig. 10 and 11, the solute concentration in the feed side, in the two types of flow pattern, increases slightly with the axial distance. The profile of the solute concentration is the same

one in both cases (Co-current and counter-current). This leads to identical variations in the solute concentrations in the permeate side (fiber side) but in an opposite way. Thus, the profiles of the solute concentration in the permeate side, in the two types of circulations, are identical and opposite. Consequently, the solvent flux which is a function of the difference of the solute concentrations on both sides of the membrane is the same, which explains the similar behavior of the modules with co-current and counter-current flow pattern.

In the case of the Co-current flow pattern, the solute concentration in the feed side and the in the permeate side increase along the module. The difference in osmotic pressure is thus more significant at the entry of the module and decreases at the exit of the module.

In the case of the counter-current, the solute concentration in the feed side increases along the module whereas the solute concentration in the permeate side (fiber side) decreases. The difference in the osmotic pressure is thus less significant at the entry of the module.

The processes of concentration or purification operate in continuous mode (with recycling). In these processes, the solute concentration in the feed flow increases with time and consequently leads to an increase in the osmotic pressure. The counter-current flow pattern module owing to the fact that in this case the difference in osmotic pressure at the entry of the module is less significant than that of the module operating co-currently, can run longer which permits the obtaining of higher rates of purity.

CONCLUSIONS

The purpose of this study has been to develop a mathematical model for reverse osmosis, to propose an efficient numerical solution procedure for the resulting set of differential model equations and highlight the importance and the efficiency of the counter-current flow pattern relative to the co-current flow pattern. The determination of the permeate flux through the membrane was based on the solution-diffusion model for both patterns. The solution procedure to solve the differential model combines the orthogonal collocation and the finite element method to obtain higher precision. The overall recovery, the feed concentration and the product concentration can be affected by the flow pattern. The overall recovery in the counter-current flow pattern is more significant. However, the improvement observed in the overall recovery, is obtained at the expense of the quality of the product obtained since its concentration also increases.

The obtained results show a similar behavior for both types of flow pattern studied. On the other hand, the counter-current module can run longer thereby improving the quality of the obtained product. The improvement achieved with the counter-current module seems insignificant because there is only one module. The use of several counter-current modules in a configuration in series - which is the case of processes on an industrial scale-allows pushing separation even further and obtaining high purity. This research attempts to gives a clear answer to the question of choosing the type of flow pattern in the reverse osmosis process especially when very high purities are required. When the reverse osmosis process is used for separation without recycling such as desalination of seawater, the two types of flow pattern can be used because they give the same results. On the other hand, in purification processes with recycling, where the objective is to achieve high purity, the counter-current flow pattern is more appropriate.

Symbols

 $A_w = Water permeability constant (h m⁻¹)$

 B_s = Solute permeability coefficient (h m⁻¹)

b⁽ⁱ⁾ = Second member of the elementary matrix in the ith element

b^G = Second member of the global matrix

C = Concentration (kg m^{-3})

 $D_m = Mean diameter (m)$

 J_s = Solute flux (kg m⁻¹ h)

 J_w = Solvent flux (kg m⁻¹ h)

 $l_i(x)$ = Lagrangian interpolation polynomial

 $M^{(i)}$ = Elementary matrix in the ith element

M^G = Global matrix in the domain

n^c = Number of internal collocation points

 ΔP = Transmembrane pressure (kg m⁻¹ h²)

Q = Volumetric flow rate $(m h^{-1})$

 \dot{Q} = Mass flow rate (kg h⁻¹)

R(x) = Residual

Sa = Membrane surface (m)

t = Time (h)

 T_R = Solute rejection

V = Volume (m)

WR_t = Water recovery

WR_{ov} = Overall recovery

 Δx = Lementary section length (m)

 $y_i^{(k)}$ = Approximation of the solution y_i at the k^{th} iteration

Greek Letters

 α = Proportionality coefficient (m h⁻¹)

 $\Delta \pi$ = Osmotic pressure difference (kg m⁻¹ h)

 $\rho_w = \text{Water density (kg m}^{-1})$

 Ω = Studied domain

 $\Omega^{(i)}$ = ith element of the domain

 $\psi_i(x)$ = Weighted functions

Subscripts

F = Feed side

f = Fiber side

P = Permeate side,

pavg = Product average concentration

R = Retentate

s = Shell side

w = Water

REFERENCES

Abbes, A., 2005. Simulation and analysis of an industrial water desalination plant. Chem. Eng. Process, 44: 999-1004.

Al-Bastaki, N.M. and A. Abbes, 1999. Modelling an industrial reverse osmosis unit. Desalination, 126: 33-39.

Al-Bastaki, N.M. and A. Abbes, 2000. Predicting the performance of reverse osmosis. Desalination, 132: 181-187.

- Al-Bastaki, N.M. and A. Abbes, 2004. Long-term performance of an industrial water desalination plant. Chem. Eng. Process, 43: 555-558.
- Araya, M.M.F., J.J. Arrieta, J.R. Pérez-Correa, L.T. Biegler and H. Jorquera, 2007. Fast and reliable calibration of solid substrate fermentation kinetic models using advanced non-linear programming techniques. Elect. J. Biotech., 10: 48-60.
- Fletcher, D.F. and D.E. Wiley, 2004. A computational fluids dynamics study of buoyancy effects in reverse osmosis. J. Membr. Sci., 245: 175-181.
- Jamal, K., M. Khan and M. Kamil, 2004. Mathematical modelling of reverse osmosis. Desalination, 160: 29-42.
- Kahdim, A.S., S.F. Ismail and A.A. Jassim, 2003. Modeling of reverse osmosis systems. Desalination, 158: 323-329.
- Lu, J., 2004. Mathematical modeling of salt-gradient ion-exchange simulated moving bed chromatography for protein separations. J. Zhejiang Univ. Sci., 5: 1613-1620.
- Mariott, J.I. and E. Sørensen, 2003. A general approach to modelling membrane module. Chem. Eng. Sci., 58: 4975-4990.
- Mariott, J.I., E. Sorensen and I.D. Bogle, 2001. Detailed mathematical modelling of membrane modules. Comp. Chem. Eng., 25: 693-700.
- Riascos, C.A.M. and J.M. Pinto, 2002. Simultaneous optimization of dynamic bioprocesses. Braz. J. Chem. Eng., 19: 449-456.
- Senthilmurugan, S., A. Ahluwalia and S.K. Gupta, 2005. Modeling of spiral-wound module and equation of model parameters using numerical techniques. Desalination, 173: 269-286.
- Slater, C.S., J.M. Zielinski, R.G. Wendel and C.G. Uchrin, 1985. Modelling of scale small reverse osmosis systems. Desalination, 52: 267-284.
- Slater, C.S. and C. Brooks, 1992. Development of a simulation model predicting performance of reverse osmosis batch systems. Sep. Sci. Technol., 27: 1388-1388.
- Tessendorf, R., R. Gani and M.L. Michelson, 1999. Modeling, simulation and optimization of membrane-based gas separation systems. Chem. Eng. Sci., 54: 943-955.
- Villadsen, J. and M.L. Michelson, 1978. Solution of Differential Equations Models by Polynomial Approximation. 1st Edn. Prentice Hall, New Jersey, USA.